UC Davis
UC Davis Previously Published Works

Title

Scapula fracture secondary to metastatic pulmonary carcinoma in a horse: Clinical, sonographic, radiographic, computed tomographic, and pathologic findings.

Permalink

https://escholarship.org/uc/item/7rd9b50p

Journal

Canadian Veterinary Journal, 61(3)

ISSN

0008-5286

Authors

Pye, Jannah
Kilcoyne, Isabelle
Roy, Melissa
et al.

Publication Date

2020-03-01

Peer reviewed

Case Report Rapport de cas

Scapula fracture secondary to metastatic pulmonary carcinoma in a horse: Clinical, sonographic, radiographic, computed tomographic, and pathologic findings

Jannah Pye, Isabelle Kilcoyne, Melissa Roy, Betsy Vaughan, Carol Ormond, Mathieu Spriet

Abstract — A 20-year-old Quarter horse gelding was referred for evaluation of an acute onset non-weight-bearing right forelimb lameness. Marked soft tissue swelling was apparent over the right scapula and shoulder region; no crepitus was palpable. A complete transverse fracture of the scapular neck was suspected based on ultrasonography and radiographs were obtained to confirm the presumptive diagnosis. A complete, oblique fracture of the right scapular neck with mild cranial and proximal displacement of the distal fragment was detected. Computed tomography of the upper right forelimb was performed post-mortem; lytic bony destruction of the scapular neck with a secondary pathologic fracture was observed. The lesion was considered most likely neoplastic. At necropsy a complete, comminuted fracture of the right scapula was confirmed, secondary to neoplastic invasion of the bone. A solitary, dorsally located, neoplastic mass was also observed within the parenchyma of the right caudal lung. Histopathologically, the lung and scapula lesions were similar, characteristic of a well-differentiated pulmonary carcinoma.

Résumé — Fracture de l'omoplate secondaire à un carcinome pulmonaire métastasique chez un cheval : trouvailles cliniques, échographiques, radiographiques, par tomodensitométrie et pathologiques. Un cheval hongre Quarter horse âgé de 20 ans fut référé pour évaluation d'une boiterie de non-appui de la patte avant droite d'apparition aiguë. Une enflure marquée des tissus mous était apparente par-dessus l'omoplate droite et la région de l'épaule; aucun crépitement n'était palpable. Une fracture transverse complète du col de l'omoplate était suspectée sur la base de l'échographie et des radiographies furent obtenues pour confirmer le diagnostic présomptif. Un examen par tomodensitométrie de la portion supérieure du membre droit fut effectué post-mortem; une destruction osseuse lytique du col de l'omoplate avec une fracture pathologique secondaire fut observée. La lésion fut considérée comme fort probablement néoplasique. Lors de la nécropsie, une fracture comminutive complète de l'omoplate droite fut confirmée, secondaire à l'invasion néoplasique de l'os. Une masse néoplasique solitaire, localisée dorsalement fut également observée dans le parenchyme du poumon caudal droit. À l'examen histopathologique, les lésions du poumon et de l'omoplate étaient similaires, caractéristiques d'un carcinome pulmonaire bien différencié.

(Traduit par Dr Serge Messier)

Tumors in the thoracic cavity of horses are uncommon and may occur as primary thoracic neoplasms or tumors that metastasize to the chest from a primary site elsewhere in the body (1–4). The incidence of primary pulmonary carcinoma is particularly low, diagnosed in only 2 of 38 horses (5.3%) with confirmed thoracic neoplasms in 1 case series (3). An antemortem diagnosis of neoplasia was not achieved in either of these 2 cases (3). The clinical manifestations of thoracic neoplasia are variable depending on the location of the tumor and the severity of the pathology (3,4). Lameness may occur secondary to bone infiltration and lysis from metastatic pulmonary neoplasia; however, fracture of the appendicular skeleton secondary to metastatic pulmonary neoplastic infiltration has not been reported (4). This case report describes a pathological fracture of the scapula in

William R. Pritchard Veterinary Medical Teaching Hospital (Pye, Roy), Department of Surgical and Radiological Sciences (Kilcoyne, Vaughan, Spriet), School of Veterinary Medicine, University of California at Davis, One Shields Avenue, Davis, California 95616, USA; Oak Hill Veterinary Services, PO Box 898, Orinda, California 94563, USA (Ormond).

Address all correspondence to Dr. Jannah Pye; e-mail: jlpye@ucdavis.edu
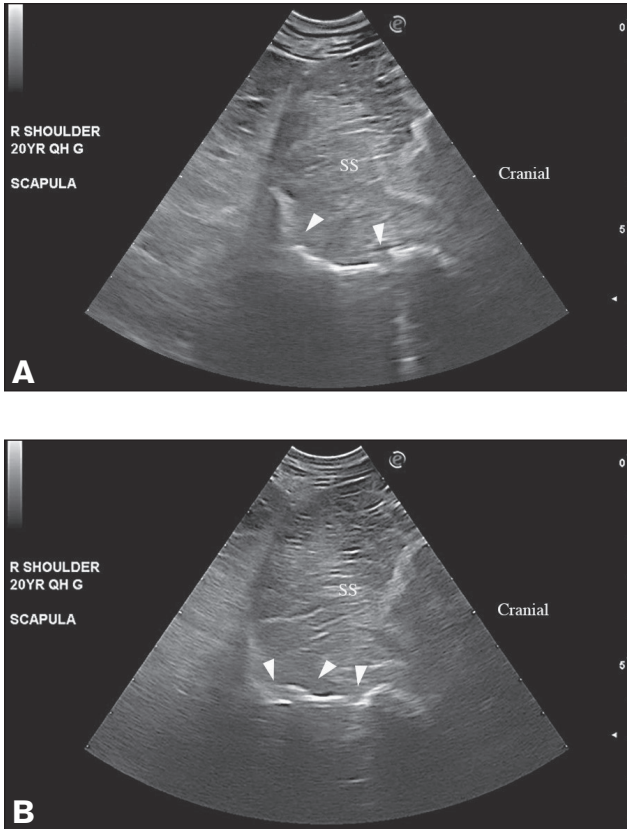
Figure 1. A – Transverse ultrasound image obtained at the level of the distal aspect of the supraspinous fossa. Step defects (arrowheads) consistent with multiple fracture lines (comminution) are seen along the width of the fossa. B – Transverse ultrasound image obtained at the level of the scapular neck revealed multiple fracture lines (arrowheads). Images obtained at 7.5 MHz with a microconvex curvilinear transducer at a depth of 9.1 cm. SS = supraspinatus muscle. Cranial is to the right.

Figure 2. Standing mediolateral radiograph of the right scapulohumeral joint showing a complete, oblique fracture of the right scapula neck.
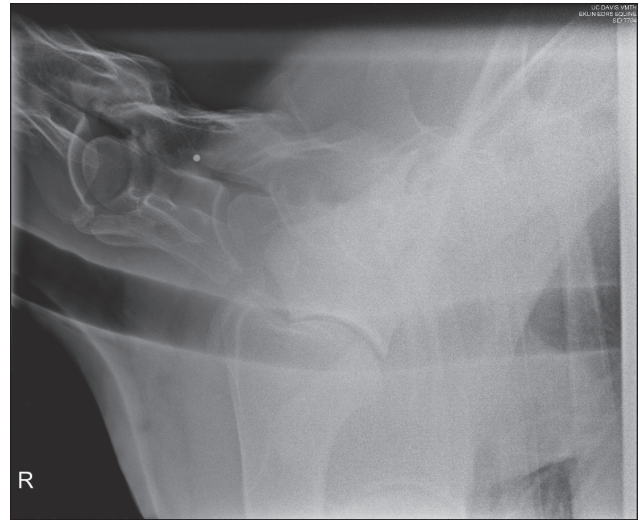
an equine patient secondary to metastatic pulmonary carcinoma. The clinical, radiological, ultrasonographic, computed tomographic, and pathological features of this neoplasm are presented.

Case description

A 20-year-old Quarter horse gelding was referred to the William R. Pritchard Veterinary Medical Teaching Hospital (VMTH) at the University of California, Davis for evaluation of an acute, severe right forelimb lameness. The gelding had stumbled on a trail ride approximately 4 h before presentation and was unable to bear weight on the right forelimb after the incident. The referring veterinarian administered flunixin meglumine, 500 mg, IV, once and referred the horse to the VMTH.

On admission, the gelding was moderately tachycardic (60 beats/min) and unwilling to walk. The horse was able to bear weight evenly on all 4 limbs when standing still, but when encouraged to walk became non-weight-bearing on the right forelimb and was unable to protract the limb. Marked soft tissue swelling was apparent over the scapula and shoulder joint, though no crepitus was palpable.

No hematological abnormalities were apparent on routine complete blood (cell) count (CBC); however, serum biochem-

istry showed moderate hypophosphatemia [1,2 mmol/L; reference range (RR): 0.68 to 1.52 mmol/L]. Ultrasonographic examination of the right scapula and scapulohumeral joint was performed. There were multiple adjacent step defects at the distal aspect of the supraspinous fossa just proximal to the neck of the scapula with cranial displacement of the fragments (Figures 1A, B). The infraspinous fossa had an irregular bony surface at the same level. The supraspinatus and infraspinatus muscles were unremarkable with the exception of intramuscular edema. The shoulder joint was mildly irregular along its articular margin. Moderate anechoic effusion was apparent within the bicipital bursa. A comminuted fracture of the distal scapula with associated intramuscular edema of the supraspinatus and infraspinatus muscles was diagnosed.

Radiographs were taken to further characterize the fracture and to investigate the possibility of concurrent humeral fracture. Standing mediolateral (Figure 2) and oblique radiographs of the right scapulohumeral joint were obtained. There was a complete, oblique fracture of the right scapula neck with mild cranial and proximal displacement of the distal fragment.

Differential diagnoses included a fracture secondary to trauma or a pathologic fracture secondary to malignant neoplasia or silicate associated osteoporosis. A poor prognosis for survival was given due to the severity of the fracture, and the owners elected euthanasia. Permission was granted by the owners for necropsy and post-mortem diagnostic tests.

Prior to necropsy, the right forelimb was separated between the scapula and the lateral thoracic wall. Computed tomography of the right scapulohumeral joint was performed. Transverse images (0.6 mm thick) of the scapula and proximal humerus in a bone algorithm were acquired. There was severe osteolysis through the proximal aspect of the neck of the scapula with complete destruction of the medial cortex and nearly complete lysis of the lateral cortex. The margins of the lytic area were poorly defined with a long zone of transition. Moderate osteoproliferation with a relatively smooth margin was identified at
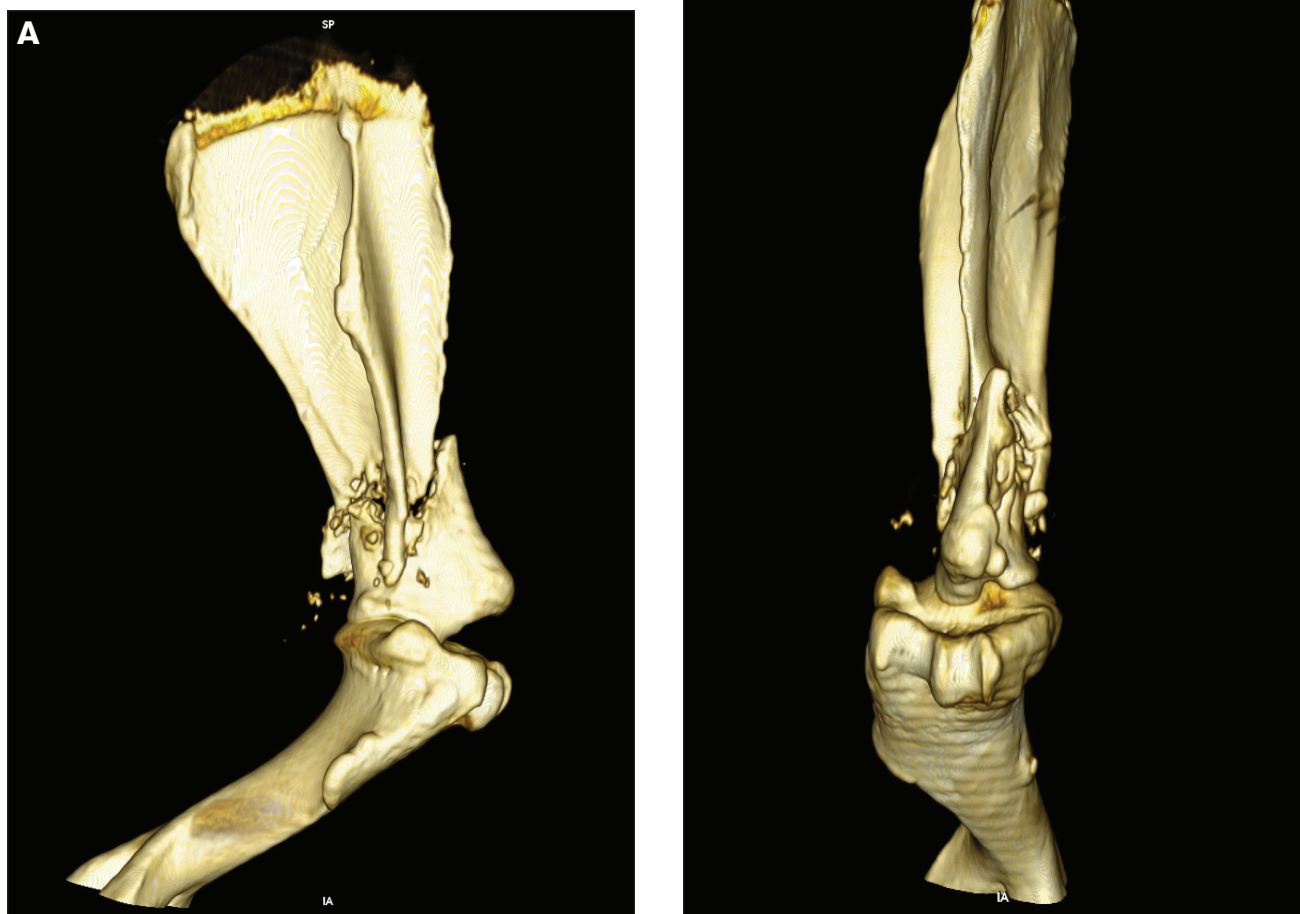
Figure 3. A – Reconstructed computed tomography image (lateromedial orientation) showing complete disruption of the cranial and caudal borders of the neck of the scapula due to a pathologic fracture. B – Reconstructed computed tomography image (craniocaudal orientation).

the medial aspect of the scapula, surrounding the area of lysis. A small amount of osteoproliferation was also present at the caudal lateral aspect of the lytic area. There was complete disruption of the cranial and caudal borders of the neck of the scapula due to a pathologic fracture (Figures 3A, B). A large cortical fragment from the caudal border, with marked resorption, was displaced caudally and distally. Small mineral fragments were present in the soft tissues at the distal aspect of this fragment. The distal part of the scapula was displaced mildly cranially and proximally. The glenoid cavity of the scapula and the proximal humerus were intact. Based on the primary destructive appearance of the scapula lesion, a neoplastic process was suspected. Osteomyelitis or an unusual focal osteolytic lesion secondary to bone fragility syndrome (Silicate Associated Osteoporosis) was considered less likely.

At necropsy, the body was found to be in good post-mortem condition and contained adequate subcutaneous and visceral adipose stores. The right scapula was sectioned transversely using a standard pathology band saw and photographed. There

was a complete, comminuted fracture with proximal displacement of the neck of the right scapula. Five variably sized comminuted bone fragments were present, the largest of which originated from the caudal aspect of the scapular wing and measured approximately 5 × 3 × 1.5 cm. Fracture fragments were hard and topographically irregular, with pitted margins. Bony proliferation was present on both cortical and medullary surfaces, and there was soft, tan, gritty tissue to soft rubbery tissue within the medullary cavity in the region of the fracture and extending into the pitted fracture margins. The surrounding soft tissues were edematous and hemorrhagic, with bone dust and countless tiny bone fragments throughout. The articular surfaces of the glenohumeral joint were mildly and irregularly eroded, with joint fluid within normal gross limits. These changes were consistent with age-related degenerative disease, unrelated to the fracture affecting the neck of the scapula.

Within the parenchyma and bulging the overlying pleura of the right caudal lung was a focal, well-demarcated, rubbery to firm, white to tan, irregularly marginated 9 × 8 × 5.5 cm
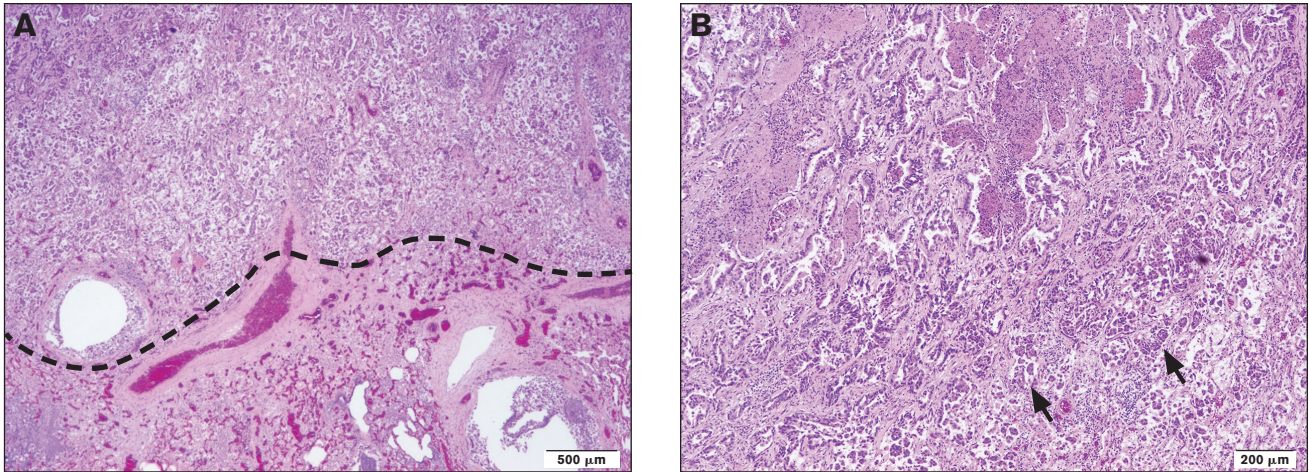
Figure 4. A – Photomicrograph of the periphery of the pulmonary mass and adjacent pulmonary parenchyma, stained with H&E at 20× magnification. The pulmonary parenchyma (below dashed line) is expanded and compressed by a mass (above dashed line) composed of neoplastic epithelial cells within dense fibrovascular stroma. B – Photomicrograph of the pulmonary mass, stained with H&E at 40× magnification. Neoplastic cells form papillary and acinar structures, as well as individual clusters and islands of cuboidal to polygonal epithelial cells (arrows).
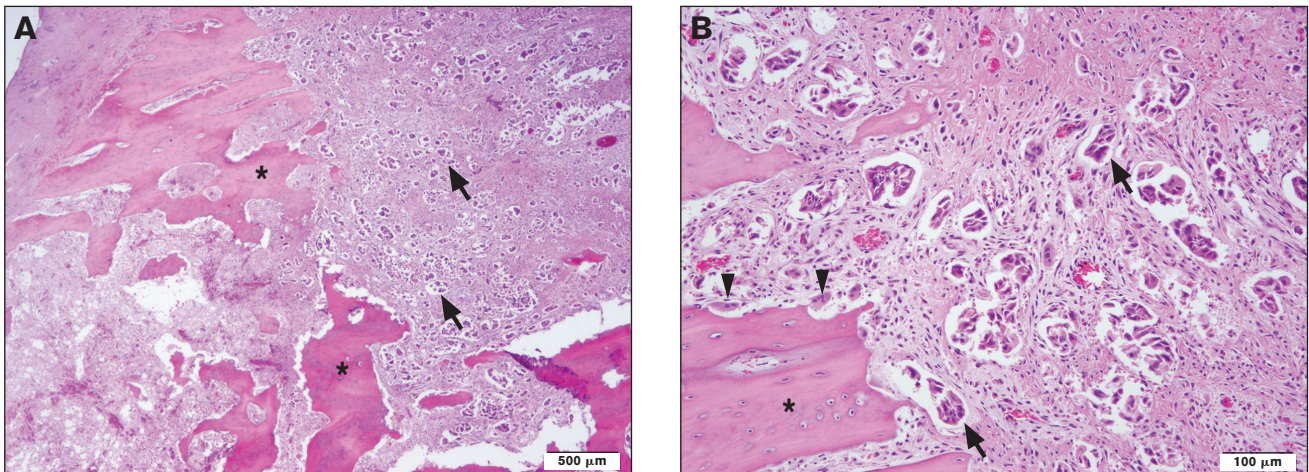
Figure 5. A – Photomicrograph of a decalcified section of the right scapula in the vicinity of the fracture, stained with H&E at 20× magnification. The bone (asterisks) is fragmented and disrupted by irregular papillary fronds and islands of pleomorphic epithelial cells (arrows) within a dense fibrovascular stroma. B – Photomicrograph of a decalcified section of the right scapula in the vicinity of the fracture, stained with H&E at 100× magnification. Fragments of bone (asterisk) have scalloped margins lined by osteoclasts (arrowheads) and are surrounded by islands of neoplastic epithelial cells (arrows).

mass. There were regions of the mass which were softer, or had a coarse, grainy texture.

Transverse tissue specimens of the right scapula and lung mass were fixed in 10% neutral buffered formalin. Subsequently, scapula tissue was demineralized in 15% formic acid. Both tissues were paraffin embedded, sectioned at 6 μm and stained with hematoxylin and eosin (H&E). Histologically, both masses were characterized as carcinomatous with tissue patterns consistent with pulmonary epithelium. The following tissues were also examined microscopically; thoracic inlet lymph node, prescapular lymph node, tonsil, kidney, spleen, liver, and heart.

The examined pulmonary tissue was composed of an infiltrative, moderately cellular, unencapsulated, well-demarcated mass composed of neoplastic epithelial cells within dense fibrovascular stroma (Figure 4A). Neoplastic cells were variably arranged in papillary and acinar patterns, and in some regions formed individual clusters and islands (Figure 4B). Individual cells were cuboidal to polygonal, had variably distinct cell margins, and contained abundant eosinophilic cytoplasm. Nuclei were round to irregularly shaped, with finely stippled chromatin and 1 to 2 nucleoli. Anisocytosis and anisokaryosis were marked, and there were 17 mitotic figures per 10 high power fields (hpf). Individual cell necrosis was common, and approximately 50% of the examined mass was necrotic. The neoplastic cells were surrounded by abundant, pale basophilic fibrovascular stroma (desmoplasia) with multifocal chondroid metaplasia, and scattered lymphocytes, plasma cells, and clumps of golden-brown pigment (hemosiderin).

Three sections of decalcified scapula were examined, in the vicinity of the pathologic fracture. Marrow spaces were filled

with large amounts of dense variably mature fibrovascular stroma punctuated by individual cells, islands, and short, irregular papillary fronds of pleomorphic epithelial cells (Figure 5A). Individual cells had variably distinct cell margins, and abundant eosinophilic cytoplasm. Nuclei were round, with finely stippled chromatin and 1 to 2 variably distinct nucleoli. Approximately 90% of the neoplastic cells and surrounding stroma were necrotic. Trabecular medullary bone was often fragmented, with scalloped edges lined by moderate numbers of osteoclasts (Figure 5B).

Discussion

The pathological diagnosis in the present case was primary pulmonary carcinoma with metastasis to the right scapula resulting in pathological fracture. Pulmonary and bronchial carcinoma and adenocarcinomas are uncommon in horses but have been described in sporadic case reports (1–3,5,6). The finding of a primary pulmonary carcinoma was unexpected due to the lack of respiratory clinical signs or any prior history indicating respiratory compromise. In previous reports of pulmonary neoplasia in horses, the presence of specific respiratory signs was dependent on the location of the tumor (3). Significant coughing was noted in 1 horse with a mediastinal mass compressing the major bronchi and trachea, whereas nodular infiltration of the parenchyma was not associated with coughing (3). Dyspnea was recorded in cases associated with pleural effusion (3). The lack of signs referable to the respiratory system in this case may be related to the location and focality of the tumor within the pulmonary parenchyma, and the lack of associated pleural effusion. Furthermore, the gelding was used for light riding only, and potentially would have displayed exercise intolerance if required to perform more strenuous work.

Metastatic tumors affecting the musculoskeletal system have been reported in horses. Tumor types known to metastasize to the skeleton include lymphosarcoma/lymphoma and hemangiosarcoma, melanoma, fibroma, squamous cell carcinoma, and adenocarcinomas (7,8). There is 1 prior report of a primary pulmonary carcinoma metastasizing to the right atrium in a Quarter horse stallion, but no record of this particular type of neoplasm metastasizing to the skeletal system in a horse (1). As in the present case, clinical presentation and laboratory abnormalities in that case report were not indicative of the primary disease but were secondary to disease caused by metastatic tumors (i.e., cardiac failure). In our case, no respiratory signs had been noted by the owners, and lameness was not observed in the affected forelimb until the occurrence of pathological fracture. However, undoubtedly the metastatic lesion had been present in the right scapula for a significant time prior to fracture.

In humans, lung cancer is one of the most diagnosed malignancies, and the majority are carcinomas (9). Among domestic animals, primary pulmonary neoplasms are encountered most frequently in older dogs and cats and rarely in other species (10). Pulmonary carcinomas in domestic animals are described broadly as either adenocarcinoma or bronchioalveolar carcinoma (11). There is significant overlap in the histologic pattern of tumors from various sites of origin within the lung, and it is often difficult to determine precise histogenesis (12). Typically, tumors derived from the large airway epithelium are more often located near the hilus of the lung, whereas tumors of parenchymal origin tend to be peripheral, as in the present case. Tumors of large airway origin predominate in humans, associated with inhalation of carcinogens, whereas tumors of the bronchioalveolar region are more common in domestic animals (12). The lung is also a frequent site for metastatic neoplasms and differentiating primary lung cancer from pulmonary metastasis resulting from malignant neoplasms elsewhere in the body can be challenging. Features supporting the diagnosis of a primary pulmonary neoplasm in this case include the presence of a single large lung mass composed of cells of epithelial origin. Most primary malignant neoplasms of the lungs appear as solitary masses of variable size that can metastasize to other areas of the lungs and to distant organs (10,12). There are no epithelial cells native to the bone, and no other neoplastic masses were found on comprehensive post-mortem examination; therefore, the pulmonary mass was considered to be primary in this case. Carcinomas in other species that are more typically affected by this particular tumor subtype commonly metastasize to the bone (e.g., transitional cell carcinoma and pulmonary carcinoma in dogs) (10).

Histologic patterns typical of progressive differentiation from a bronchioloalveolar pattern (papillary and acinar patterns) were noted in this case, consistent with a primary lung tumor (12). Also, the spectrum of progression of neoplastic transformation noted within the lung mass is suggestive of a primary tumor, as metastases tend to be more uniformly differentiated (12). Arguably, immunohistochemical staining could have been performed to support the histopathological diagnosis. Pancytokeratin immunohistochemical staining can distinguish epithelial from mesenchymal differentiation and may have been used to demonstrate the epithelial origin of the neoplastic scapula cells (13). Detection of thyroid transcription factor-1 by immunohistochemistry could have been used as an additional confirmatory test, as it is specific for tumors of bronchioloalveolar origin (11,12).

This case highlights the fact that equine pulmonary carcinoma may metastasize to the appendicular skeleton, eventually resulting in catastrophic fracture. Horses affected by metastatic pulmonary carcinoma may show few or no preceding clinical signs of the primary disease or the metastatic process. Full necropsy is recommended whenever possible to identify metastatic disease which may not be clinically apparent.   CVJ

References

1. Dill S, Moise NS, Meschter CL. Cardiac failure in a stallion secondary to metastasis of an anaplastic pulmonary carcinoma. Equine Vet J 1986;18:414–417.
2. Uphoff CS, Lyncoln JA. A primary pulmonary tumour in a horse. Equine Pract 1987;9:19–20.
3. Mair TS, Brown PJ. Clinical and pathological features of thoracic neoplasia in the horse. Equine Vet J 1993;25:220–223.
4. Mair TS, Rush BR, Tucker RL. Clinical and diagnostic features of thoracic neoplasia in the horse. Equine Vet Educ 2004;16:30–36.
5. Van Rensburg IBJ, Stadler P, Soley J. Bronchiolo-alveolar adenocarcinoma in a horse. J S Afr Vet Assoc 1989;60:212–214.
6. Anderson JD, Leonard JM, Zeliff JA, Garman RH. Primary pulmonary neoplasm in a horse. J Am Vet Med Assoc 1992;201:1399–1401.
7. Rush-Moore B, Weisbrode SE, Biller DS, Williams J. Metacarpal fracture associated with lymphosarcoma-induced osteolysis in a horse. J Am Vet Med Assoc 1995;207:208–210.

8. Southwood LL, Schott HC, Henry CJ, et al. Disseminated hemangiosarcoma in the horse: 35 cases. J Vet Intern Med 2000;12:105–109.
9. Husain AN. The lung. In: Kumar V, Abbas AK, Aster JC, eds. Pathologic Basis of Disease. 9th ed. London, UK: Elsevier Saunders, 2015:669–726.
10. Lopez A, Martinson SA. Respiratory system, mediastinum and pleurae. In: Zachary JF, ed. Pathologic Basis of Veterinary Disease. 6th ed. St. Louis, Missouri: Elsevier, 2017:471–560.

11. Caswell LJ, Williams KJ. Respiratory system. In: Grant MM, ed. Jubb, Kennedy & Palmer's Pathology of Domestic Animals. 5th ed. Edinburgh, UK: Elsevier, 2007:495–474.
12. Wilson DW. Tumors of the respiratory tract. In: Meuten D, ed. Tumors in Domestic Animals. 5th ed. Ames, Iowa: John Wiley and Sons, 2017: 467–498.
13. Painter JT, Clayton NP, Herbert RA. Useful immunohistochemical markers of tumor differentiation. Toxicol Pathol 2010;38:131–141.